Balancing Source Terms and Flux Gradients in High-Resolution Godunov Methods: The Quasi-Steady Wave-Propogation Algorithm

Randall J. LeVeque[1]

Abstract. Conservation laws with source terms often have steady states in which the flux gradients are nonzero but exactly balanced by source terms. Many numerical methods (*e.g.*, fractional step methods) have difficulty preserving such steady states and cannot accurately calculate small perturbations of such states. Here a variant of the wave-propagation algorithm is developed which addresses this problem by introducing a Riemann problem in the center of each grid cell whose flux difference exactly cancels the source term. This leads to modified Riemann problems at the cell edges in which the jump now corresponds to perturbations from the steady state. Computing waves and limiters based on the solution to these Riemann problems gives high-resolution results. The 1D and 2D shallow water equations for flow over arbitrary bottom topography are use as an example, though the ideas apply to many other systems. The method is easily implemented in the software package CLAWPACK.

Keywords: Godunov methods, shock capturing, source terms, conservation laws, steady states, shallow water equations.

AMS Classification: 65M06, 76M20

Running head: Balancing Source Terms and Flux Gradients

1 Introduction

We consider the conservation law

$$q_t + f(q)_x = \psi(q) \tag{1}$$

and its multidimensional analogue, where f is the flux function and $\psi(q)$ is a source term. For the homogeneous conservation law (with $\psi \equiv 0$), many high-resolution numerical methods have been developed that are second-order accurate on smooth solutions and which give sharp resolution of discontinuities in the solution such as shock waves. Here we are particularly concerned with the wave-propagation algorithms developed in [11], Godunov-type finite-volume methods in which Riemann problems are solved at cell interfaces to properly resolve the wave structure. These waves are used both for making the first-order Godunov update and for implementing second-order correction terms, typically with the application of limiters to suppress oscillations. In multi-dimensional problems, a transverse splitting of the waves is also used to improve stability and resolution (see also [10] for a general discussion of such methods).

For equations with source terms, the simplest approach is to use a fractional step splitting method, in which one alternates between solving the homogeneous conservation law

$$q_t + f(q)_x = 0 \tag{2}$$

[1]Department of Applied Mathematics and Department of Mathematics, University of Washington, Box 352420, Seattle, WA 98195-2420. `rjl@amath.washington.edu`

Version of January 9, 1998.

and the ordinary differential equation

$$q_t = \psi(q) \tag{3}$$

in each time step, avoiding the necessity of incorporating source terms into the high-resolution method. For many problems this approach is quite successful. For some types of problems, however, fractional step methods perform quite poorly. In particular, this is true for problems where q_t is small relative to $f(q)_x$ and $\psi(q)$, so that the solution is close to a steady state in which the flux gradient $f(q)_x$ and the source term $\psi(q)$ should exactly balance. Accurate solution of such steady-states, and of time-dependent dynamical perturbations (*quasi-steady solutions*) relies on the numerical method respecting this delicate balance. Fractional step methods can easily fail since solving (2) may lead to large changes in the solution which should then be exactly undone by solving (3). It is unlikely that this will happen exactly, especially since very different sorts of numerical methods are used in the two steps. Even if there were exact cancellation for a steady state, small dynamical perturbations can easily be reduced to noise in the process of making these changes and counterchanges which may be orders of magnitude larger than the perturbation of interest.

In this paper an approach is developed which allows the source term to be easily incorporated into the wave-propagation algorithm, avoiding fractional steps. This allows small perturbations in quasi-steady problems to be computed with the same high resolution as would be expected if calculating small perturbations about a constant state with the homogeneous equation. With this approach the Riemann solvers and limiters are, in essence, applied directly to the perturbations. This approach will be called the *quasi-steady wave-propagation algorithm*, and is developed here in both one and two space dimensions in the context of the shallow water equations.

Overview. Godunov's method and the wave-propagation algorithm of [11] are based on viewing the finite-volume cell average in each time step as defining a piecewise constant function with constant value Q_i in the i'th grid cell. Solving the *Riemann problem* between Q_{i-1} and Q_i at a cell interface gives a set of waves which affect both of the cell averages over the next time step. This is described in slightly more detail in Section 2, but familiarity with [11] is assumed.

The basic idea explored here is to introduce a new discontinuity in the center of each grid cell at the start of each time step, with value Q_i^- on the left half of the cell and Q_i^+ on the right half. These values are chosen so that

$$\frac{1}{2}(Q_i^- + Q_i^+) = Q_i \tag{4}$$

and also, if possible, that

$$f(Q_i^+) - f(Q_i^-) = \psi(Q_i)\Delta x. \tag{5}$$

The condition (4) guarantees that the cell average is unchanged by the modification, while (5), if satisfied, means that the waves resulting from solving the Riemann problem at this new discontinuity will exactly cancel the effect of the source term in this cell. See Section 2 for more discussion of this. Hence it is not necessary to solve this newly-introduced Riemann problem or deal with the resulting waves in the algorithm, nor is it necessary to apply the source term any longer. By ignoring both, we respect the steady state balance inherent in the equations. (Note that (5) is a discrete version of $f(q)_x = \psi(q)$.)

We must still solve Riemann problems at the cell interfaces, but these are now between modified states Q_{i-1}^{+} and Q_i^{-} rather than between Q_{i-1} and Q_i (see Figure 2). If the solution is quasi-steady then $Q_{i-1}^{+} \approx Q_i^{-}$ (whereas Q_{i-1} and Q_i might have had a large jump between them if the steady state solution has rapid spatial variation, leading to "strong" waves in the Riemann solution). By solving the Riemann problem between Q_{i-1}^{+} and Q_i^{-} we are working directly with the perturbations from steady state, as desired. The resulting "weak" waves modify the cell averages by small amounts corresponding directly to the dynamic perturbations, rather than making larger changes based on strong waves which must later be undone by the source terms. Moreover, the second-order correction terms are also computed directly from these weak waves, and limiters are applied directly to these waves. By contrast, in a fractional step approach the limiters are applied to the strong waves coming from the original data, and if these are rapidly varying then the limiting procedure can lead to a complete corruption of the small amplitude perturbations of interest.

This approach is described more formally and in greater detail starting in Section 2. The relation of this approach to other methods commonly used to handle such problems without splitting the equations is explored in Section 4.

Applications. Quasi-steady problems arise in many applications. Some examples include:

- Shallow water equations with source terms arising from bottom topography, *e.g.*, flow in a one-dimensional channel with an irregular bottom. Many practical problems involving the two-dimensional shallow water equations in oceanography or atmospheric science require the inclusion of bottom topography.
- Gas dynamics with geometrical source terms, such as the quasi-one-dimensional nozzle.
- Fluid dynamics with gravity, eigher a constant gravitational field as in atmospheric problems, or self-gravity, as in modeling stellar dynamics, for example. Often it is of interest to model perturbations which are small relative to the underlying variations in density and pressure arising from the gravitational force.

An example of this approach for the one-dimensional isothermal Euler equations in a gravitational field was given in [12]. More extensive tests are currently underway for the full multi-dimensional Euler equations in the presence of gravity.

In this paper the shallow water equations (in 1 and 2 dimensions) will be used as an example. The shallow water equations have the advantage of being a relatively simple system where the ideas are easy to explain and interpret physically. With this example it is also possible to put in any reasonable bottom topography and have a physically meaningful test problem, which is not the case with gravitational source terms, for example, where only certain forms of the source term make sense. Hence the approach can be subjected to a wider variety of tests. The shallow water equations with bottom topography are also extremely important in their own right.

2 Godunov's method

Let $Q_i \equiv Q_i^n$ denote cell averages at time t_n and let $\bar{Q}_i \equiv Q_i^{n+1}$ be the updated cell averages at time t_{n+1}. (We suppress superscripts since all the methods discussed are one-step methods and other superscripts will be needed below.) Godunov's method for the homogeneous conservation law (2) is derived by viewing the data at time t_n as defining a piecewise constant function with value Q_i in the i'th cell and jump discontinuities at the cell interfaces $x_{i-1/2}$, as shown in Figure 1(a). Solving the Riemann problems at the interfaces gives rise to waves propagating in the x-t plane as indicated in Figure 1(b). If $Q^*_{i-1/2}$ denotes the value of the Riemann solution along the interface $x_{i-1/2}$ for $t > t_n$, then Godunov's method can be written as

$$\begin{aligned}\bar{Q}_i &= Q_i - \frac{\Delta t}{\Delta x}(f(Q^*_{i+1/2}) - f(Q^*_{i-1/2})) \\ &= Q_i - \frac{\Delta t}{\Delta x}(\mathcal{A}^+\Delta Q_{i-1/2} - \mathcal{A}^-\Delta Q_{i+1/2})\end{aligned} \tag{6}$$

where the notation of [11] is used for flux differences,

$$\begin{aligned}\mathcal{A}^+\Delta Q_{i-1/2} &= f(Q_i) - f(Q^*_{i-1/2}) \\ \mathcal{A}^-\Delta Q_{i+1/2} &= f(Q^*_{i+1/2}) - f(Q_i).\end{aligned} \tag{7}$$

Note, however, that the notation of [11] has been modified here to use $i - 1/2$ as the index for the interface between cells $i - 1$ and i (rather than using i for this index). In this paper it will be important to make distinctions between edge values and cell-centered values.

Solving the Riemann problem at $x_{i-1/2}$ gives a flux difference splitting

$$f(Q_i) - f(Q_{i-1}) = \mathcal{A}^-\Delta Q_{i-1/2} + \mathcal{A}^+\Delta Q_{i-1/2}. \tag{8}$$

The right-going portion $\mathcal{A}^+\Delta Q_{i-1/2}$ modifies the cell average Q_i while the left-going portion $\mathcal{A}^-\Delta Q_{i-1/2}$ modifies the cell average Q_{i-1}.

Now suppose we replace the constant value Q_i in Figure 1 by two values Q_i^- and Q_i^+ with a jump at the cell center, as shown in Figure 2(a). If Q_i^+ and Q_i^- are chosen as

$$\begin{aligned}Q_i^- &= Q_i - \delta_i \\ Q_i^+ &= Q_i + \delta_i\end{aligned} \tag{9}$$

for some vector δ_i, then (4) will be satisfied and total mass will be preserved. If we now apply the idea of Godunov's method, advancing forward in time for this piecewise constant data, we obtain the x-t structure shown in Figure 2(b). In addition to the Riemann problems at the cell edges, there is a Riemann problem to be solved at the cell center which also leads to a set of waves. For a sufficiently small time step Δt, (small enough that the Courant number is less than 1/2), the waves remain entirely within the i'th cell. The cell average is now updated by the incoming waves from each cell edge, as before, and also by *all* the waves from the Riemann problem at the cell center, since they all remain in this cell. As a result, we do not need to actually solve this Riemann problem to split the flux difference $f(Q_i^+) - f(Q_i^-)$ into left-going and right-going pieces, since both will be used to update the cell average. If we continue to denote the flux-difference splitting at the cell interfaces by $\mathcal{A}^+\Delta Q_{i-1/2}$ (incoming waves from the left edge, arising from solving the Riemann problem between Q_{i-1}^+ and Q_i^-) and $\mathcal{A}^-\Delta Q_{i+1/2}$ (incoming waves from the right edge), then the full update formula is now

$$\bar{Q}_i = Q_i - \frac{\Delta t}{\Delta x}(\mathcal{A}^+\Delta Q_{i-1/2} - \mathcal{A}^-\Delta Q_{i+1/2}) - \frac{\Delta t}{\Delta x}(f(Q_i^+) - f(Q_i^-)). \tag{10}$$

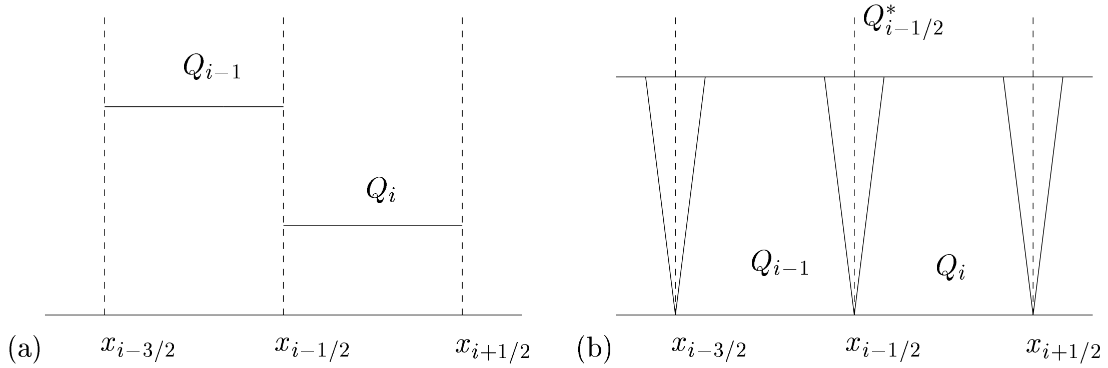

Figure 1: (a) Data in two adjacent grid cells, viewed as defining a piecewise constant function for Godunov's method. (b) Structure of the solution to the resulting Riemann problems, as seen in the x-t plane.

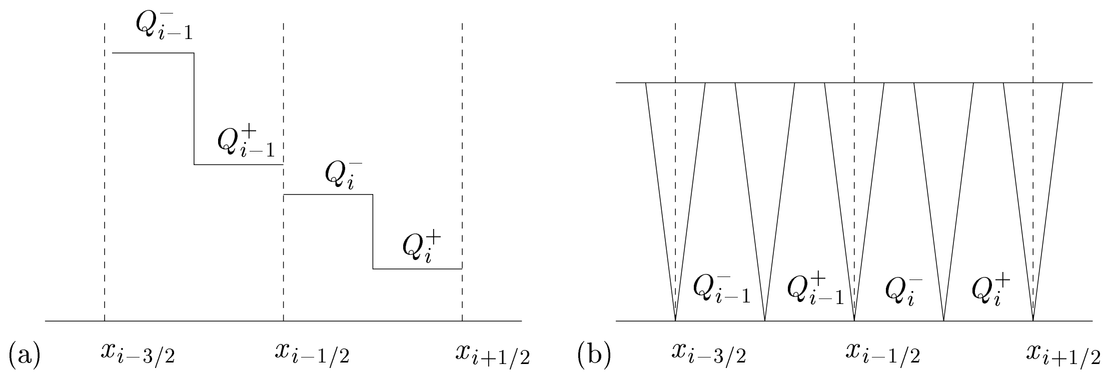

Figure 2: (a) The same data in two adjacent grid cells as in Figure 1, after introducing a jump δ in the center of each grid cell for the quasi-steady method. (b) Structure of the solution to the resulting Riemann problems, as seen in the x-t plane.

Now suppose there is a source term $\psi(q)$ in the equation, giving (1). Then a simple first-order unsplit method results from taking the Godunov update (10) and also adding in $\Delta t\psi(Q_i)$, the source contribution over time Δt. Adding this to (10) results in

$$\bar{Q}_i = Q_i - \frac{\Delta t}{\Delta x}(\mathcal{A}^+\Delta Q_{i-1/2} - \mathcal{A}^-\Delta Q_{i+1/2}) + \Delta t\left[\psi(Q_i) - \frac{1}{\Delta x}(f(Q_i^+) - (Q_i^-))\right]. \tag{11}$$

If we can choose δ_i in (10) so that (5) is satisfied, then the final term here drops out and we have a method that looks identical to the original Godunov method (6), but with the flux difference splitting $\mathcal{A}^{\pm}\Delta Q_{i-1/2}$ determined by solving the Riemann problems with data Q_{i-1}^+ and Q_i^- rather than the original Q_{i-1} and Q_i.

3 High-resolution methods

Solving the Riemann problem between states Q_{i-1}^+ and Q_i^- results in a set of waves $\mathcal{W}_{i-1/2}^p$ propagating at speeds $\lambda_{i-1/2}^p$, for $p = 1,\ 2,\ \dots,\ m$ (again following the notation of [11] but with index $i-1/2$ in place of i). The Godunov method is extended to a high-resolution method by adding in correction terms to obtain

$$\bar{Q}_i = Q_i - \frac{\Delta t}{\Delta x}(\mathcal{A}^+\Delta Q_{i-1/2} - \mathcal{A}^-\Delta Q_{i+1/2}) - \frac{\Delta t}{\Delta x}(\tilde{F}_{i+1/2} - \tilde{F}_{i-1/2}),$$

where

$$\tilde{F}_{i-1/2} = \frac{1}{2}\sum_{p=1}^{m} |\lambda_{i-1/2}^p| \left(1 - \frac{\Delta t}{\Delta x}|\lambda_{i-1/2}^p|\right)\tilde{\mathcal{W}}_{i+1/2}.$$

Here $\tilde{\mathcal{W}}_{i+1/2}$ is a limited version of the wave $\mathcal{W}_{i-1/2}^p$, obtained by comparing $\mathcal{W}_{i-1/2}^p$ to the corresponding p-wave at the adjacent Riemann problem in the upwind direction, based on the sign of $\lambda_{i-1/2}^p$. Hence

$$\tilde{\mathcal{W}}_{i+1/2} = \text{limiter}(\mathcal{W}_{i-1/2}^p, \mathcal{W}_{I-1/2}^p),$$

where

$$I = \begin{cases} i-1 & \text{if } \lambda_{i-1/2}^p > 0 \\ i+1 & \text{if } \lambda_{i-1/2}^p < 0. \end{cases}$$

See [11] for more details and some specific limiters. (The MC limiter is used in all examples below.)

These high-resolution corrections are unchanged when source terms are included. But since the waves $\mathcal{W}_{i-1/2}^p$ are now calculated based on the modified values Q_{i-1}^+ and Q_i^-, these corrections have small magnitude. Moreover the limiters are applied directly to these perturbations to the steady state.

4 Linear systems

First consider the linear hyperoblic system with a (possibly nonlinear) source term,

$$q_t + Aq_x = \psi(q). \tag{12}$$

We assume that ψ is a smooth function of q, and also that A is nonsingular (see Section 5.1 for some comments on the case where A is singular). Then any steady state solution is smooth and satisfies

$$q_x = A^{-1}\psi(q), \tag{13}$$

together with appropriate boundary conditions.

When A is nonsingular, the condition (5) can always be satisfied in each grid cell for the system (12). Given a state Q_i we need to find δ_i so that $Q_i^- = Q_i - \delta_i$ and $Q_i^+ = Q_i + \delta_i$ satisfy

$$A(Q_i^+ - Q_i^-) = \Delta x\, \psi(Q_i),$$

which leads to

$$\delta_i = \frac{\Delta x}{2} A^{-1}\psi(Q_i). \tag{14}$$

For the linear system, the Riemann problem can be explicitly solved in terms of the eigenstructure of A. Let

$$A = R\Lambda R^{-1},$$

where $\Lambda = \text{diag}(\lambda^p)$ is the matrix of eigenvectors and

$$R = [r^1|r^2|\cdots|r^m]$$

is the matrix of right eigenvectors, so $Ar^p = \lambda^p r^p$. Let $\lambda^+ = \max(\lambda, 0)$, $\lambda^- = \min(\lambda, 0)$, and set

$$\begin{aligned} \Lambda^\pm &= \text{diag}((\lambda^p)^\pm), \\ A^\pm &= R\Lambda^\pm R^{-1} \end{aligned} \tag{15}$$

so that $A = A^+ + A^-$ gives a splitting of A into pieces with nonnegative eigenvalues and pieces with nonpositive eigenvalues respectively.

For the homogeneous problem with $\psi \equiv 0$, Godunov's mehod reduces to

$$\bar{Q}_i = Q_i - \frac{\Delta t}{\Delta x}\left(A^+(Q_i - Q_{i-1}) + A^-(Q_{i+1} - Q_i)\right).$$

This is simply the upwind method. The waves $\mathcal{W}^p_{i-1/2}$ are eigenvectors of A, and if no limiters are used then the high-resolution correction reduces to

$$\begin{aligned} \tilde{F}_{i-1/2} &= \frac{1}{2}|A|\left(1 - \frac{\Delta t}{\Delta x}|A|\right)(Q_i - Q_{i-1}) \\ &= \frac{1}{2}\left(|A| - \frac{\Delta t}{\Delta x}A^2\right)(Q_i - Q_{i-1}) \end{aligned} \tag{16}$$

where

$$|A| = A^+ - A^- = R|\Lambda|R^{-1}.$$

When these corrections are added into the upwind method, we obtain the standard Lax-Wendroff method.

Now suppose there is a source term and we choose δ_i as in (14) so that this source term is exactly cancelled. Godunov's method as extended in Section 2 then becomes

$$\bar{Q}_i = Q_i - \frac{\Delta t}{\Delta x}\left(A^+(Q_i^- - Q_{i-1}^+) + A^-(Q_{i+1}^- - Q_i^+)\right).$$

Using $Q_i^\pm = Q_i \pm \delta_i$ in this expression and rearranging terms shows that

$$\bar{Q}_i = Q_i - \frac{\Delta t}{\Delta x}\left(A^+(Q_i - Q_{i-1}) + A^-(Q_{i+1} - Q_i)\right) + \Delta t(A^+A^{-1}\psi_{i-1/2} + A^-A^{-1}\psi_{i+1/2}), \tag{17}$$

where

$$\psi_{i-1/2} = \frac{1}{2}(\psi(Q_{i-1}) + \psi(Q_i)).$$

Hence, for the linear system, this method is equivalent to applying the upwind method to the original data but with a first-order approximation to the source term also included. Note that

$$A^+A^{-1} + A^-A^{-1} = (A^+ + A^-)A^{-1} = I,$$

so that this term in (17) does give a consistent approximation to $\Delta t\psi(Q_i)$. This term can also be interpreted as follows: $\psi_{i-1/2}$ is an approximation to the source term at $x_{i-1/2}$, which is split into two pieces $A^-A^{-1}\psi_{i-1/2}$ and $A^+A^{-1}\psi_{i-1/2}$ (which sum to $\psi_{i-1/2}$). The first piece is used to modify Q_{i-1} while the latter modifies Q_i. This amounts to projecting $\psi_{i-1/2}$ onto the right-going characteristics to compute the portion updating Q_i and onto the left-going characteristics to compute the portion updating Q_{i-1}. This approach is often used for source terms (*e.g.*, [2], [13], [14]) even for nonlinear problems, in which case eigenstructure of the Roe matrix at $x_{i-1/2}$ might be used to split $\psi_{i-1/2}$, for example.

The approach suggested here is somewhat different for nonlinear problems, however. In particular, it yields a simple and effective extension from Godunov's method to the inclusion of high-resolution correction terms.

Another approach which has been explored in the literature (*e.g.*, [3], [4], [5], [15]) is to use a piecewise linear reconstruction within each grid cell, choosing the slope in such a way that $f(q)_x \approx \psi(Q_i)$ within the i'th cell. The approach introduced here is similar, but the source-balancing slope is now concentrated into a delta function at the center of the cell, and the resulting jumps at cell interfaces define slopes (actually waves) which can be used for second-order corrections in the usual manner.

Greenberg and LeRoux [6] proposed a method for scalar equations that is also related to the quasi-steady wave-propagation approach, though only first-order accurate. Some other approaches to this problem can be found in [1], [7], [16],

5 The shallow water equations

As an example of how this technique can be applied to nonlinear systems, we consider the shallow water equations with bottom topography in both one and two dimensions. First consider flow in a one-dimensional channel with the bottom elevation given by $B(x)$. Let $h(x,t)$ represent the fluid depth above this bottom, so the top surface is at $B(x) + h(x,t)$, and let $u(x,t)$ be the velocity. Then the equations are

$$\begin{aligned} h_t + (hu)_x &= 0 & (18) \\ (hu)_t + \left(hu^2 + \frac{1}{2}gh^2\right)_x &= -ghB_x & (19) \end{aligned}$$

where g is the gravitational constant and $B_x = B'(x)$.

One steady-state solution is obtrained by assuming there is no motion ($u \equiv 0$) and the top surface is flat, so $h(x,t) = 1 - B(x)$ for some constant C, which will always be taken to be 1 below. Suppose we wish to compute small perturbations of this steady state.

Let $Q_i = [h_i, (hu)_i]$ be the state in the i'th grid cell. Since there is no source term in the equation (18), the momentum hu must be continuous across the new discontinuity introduced at the cell center. Let $m_i = (hu)_i$ denote this value. We need only determine the jump in h to be introduced, so we wish to find a scalar value δ_i so that

$$h_i^{\pm} = h_i \pm \delta_i \tag{20}$$

satisfy

$$\left(m_i^2/h_i^+ + \frac{1}{2}g(h_i^+)^2\right) - \left(m_i^2/h_i^- + \frac{1}{2}g(h_i^-)^2\right) = -ghB_x\Delta x, \tag{21}$$

where we have used $hu^2 = (hu)^2/h$. We suppose that the bottom topography $B(x)$ is specified as cell edge values $B_{i-1/2}$ and use $B_{i+1/2} - B_{i-1/2} \equiv \Delta B_i$ on the right hand side in place of $B_x\Delta x$. Inserting (20) in (21) and simplifying gives

$$m_i^2\left(\frac{1}{h_i+\delta_i} - \frac{1}{h_i-\delta_i}\right) + gh_i(2\delta_i + \Delta B_i) = 0. \tag{22}$$

Clearing the denominator results in a cubic equation for δ_i, which always has at least one real root. For the case we are now considering, small perturbations about $u \equiv 0$, we will have $m_i \approx 0$ and so

$$\delta_i \approx -\frac{1}{2}\Delta B_i.$$

A simple Newton iteration quickly converges to the appropriate solution of (22) in this case.

Note in particular that if we are simply trying to preserve the steady state numerically, this approach works perfectly and keeps the top surface flat. Given values $B_{i-1/2}$, take $h_i = 1 - \frac{1}{2}(B_{i-1/2} + B_{i+1/2})$ and $m_i = 0$ as initial data. Then (22) gives $\delta_i = -\frac{1}{2}\Delta B_i$ so that

$$h_i^- = h_i - \delta_i = B_{i-1/2}.$$

A similar calculation in cell $i-1$ shows that

$$h_{i-1}^+ = h_{i-1} + \delta_{i-1} = B_{i-1/2}$$

also. So the resulting Riemann problem at $x_{i-1/2}$ has no jump, and this steady state is exactly preserved. A fractional step method would not in general preserve this steady state.

Example 5.1. As bottom topography take

$$B(x) = \begin{cases} 0.25(\cos(\pi(x-0.5)/0.1)+1) & \text{if } |x-0.5| < 0.1 \\ 0 & \text{otherwise} \end{cases} \tag{23}$$

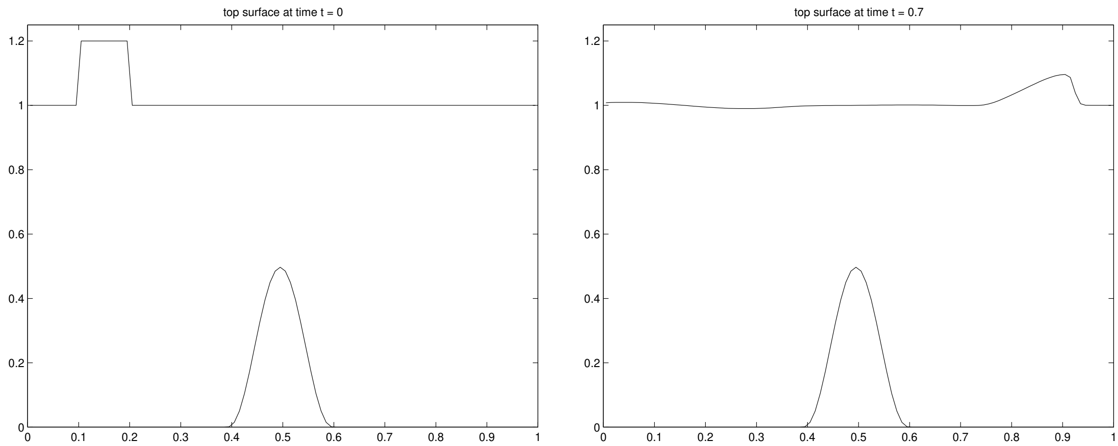

Figure 3: Bottom topography and top surface for the one-dimensional shallow water equations of Example 5.1 in the case $\epsilon = 0.2$. At time $t = 0.7$ the right-going portion of the pulse has moved past the hump. A magnified view of this solution is shown in Figure 4 (bottom right).

on $0 < x < 1$ with $C = 1$ and $g = 1$. This hump has height 0.5, as shown in Figure 3. The initial data is the stationary solution $m_i \equiv 0$ and $h_i = 1 - \frac{1}{2}(B_{i-1/2} + B_{i+1/2})$, with a small perturbation

$$h_i \;:=\; h_i + \epsilon \text{ for } 0.1 < x < 0.2.$$

This disturbance splits into two waves which, for small ϵ, are essentially linear waves propagating at the characteristic speeds $\pm\sqrt{gh}$. The left-going wave leaves the domain (zero-order extrapolation boundary conditions are used [11]) and the right-going wave moves through the region where B varies. Figure 4 shows the computed surface $h_i + \frac{1}{2}(B_{i-1/2} + B_{i+1/2})$ at time $t = 0.7$, compared to a fine grid "exact" solution. Results are shown for both $\epsilon = 0.2$ and $\epsilon = 10^{-3}$ with both the fractional step method and the approach developed above, using the high-resolution method with the MC limiter in each case.

The fractional step method does not preserve this steady state and gives perturbations of the top surface that are of magnitude roughly 10^{-3} over the region where $B(x)$ is nonzero. For $\epsilon = 10^{-3}$ the disturbance we are attempting to model is of the same magnitude as this error. In this example the topography is nonzero only over $0.4 < x < 0.6$ and at the time shown the disturbance has passed this region and so can be easily distinguished. At an earlier time, or in a problem where H varies everywhere, the wave of interest would be lost in the noise.

When the disturbance is larger, $\epsilon = 0.2$, the wave (which now steepens nonlinearly) is well above the noise level, but the effect of the bottom topography is still visible.

With the approach developed here the resolution of the pulse is equally good for both values of ϵ, and as good as one would expect in the homogeneous case $B(x) \equiv 0$.

5.1 Steady flow.

There are other steady states besides the stationary state with $u \equiv 0$, consisting of steady flow in which the momentum m is constant in x but nonzero. There are several different regimes of such flow, depending on the bottom topography and the free-stream Froude number $Fr = u/\sqrt{gh}$ (analogous to the Mach number in compressible gas dynamics). See [8] for a

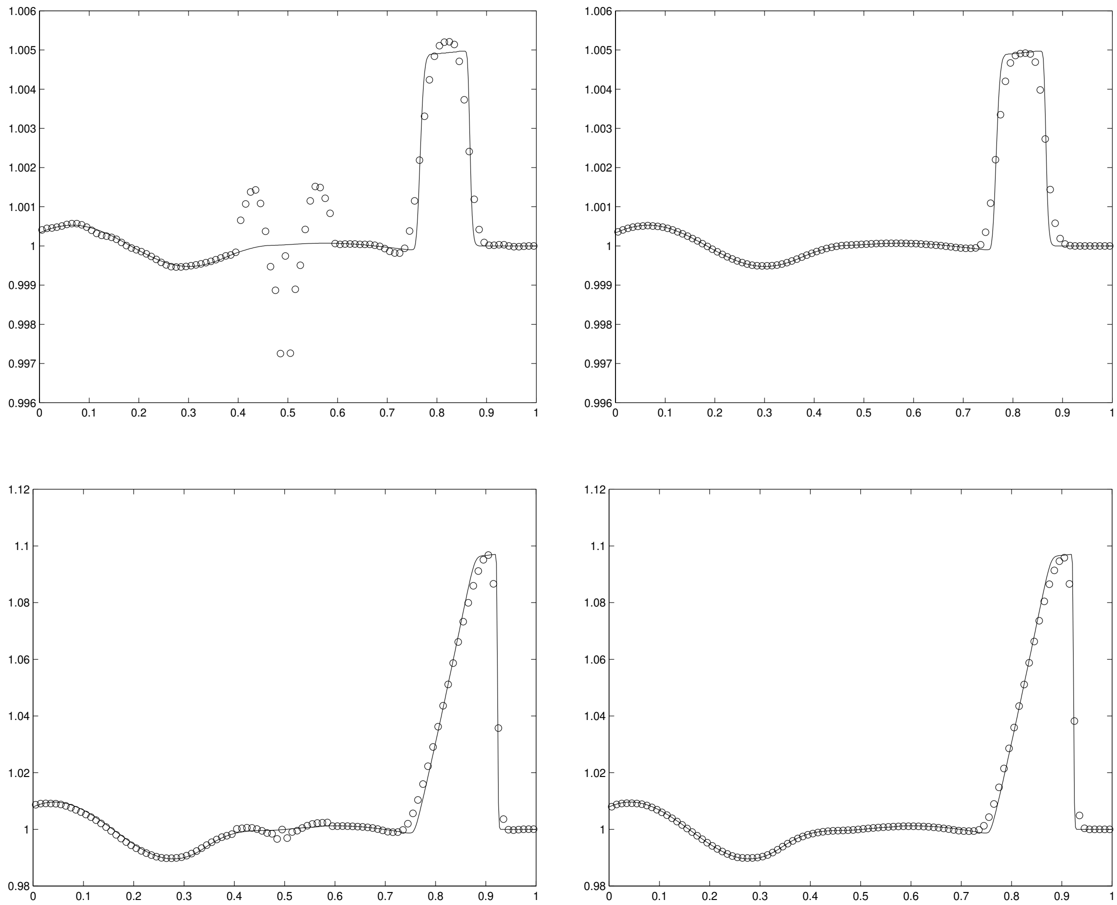

Figure 4: Comparison of computed results for flow over the hump shown in Figure 3. Results are shown using the fractional step method (left column) and the quasi-steady wave-propagation method (right column). The water surface is shown at time $t = 0.7$ for two values of ϵ, the initial perturbation of the surface: $\epsilon = 10^{-3}$ (top figures) and $\epsilon = 0.2$ (bottom figures). The right-going pulse has moved past the hump and also been partially reflected by the hump, giving the disturbance seen on the left. The solid curve in each case is a reference solution computed with the quasi-steady method on a much finer grid.

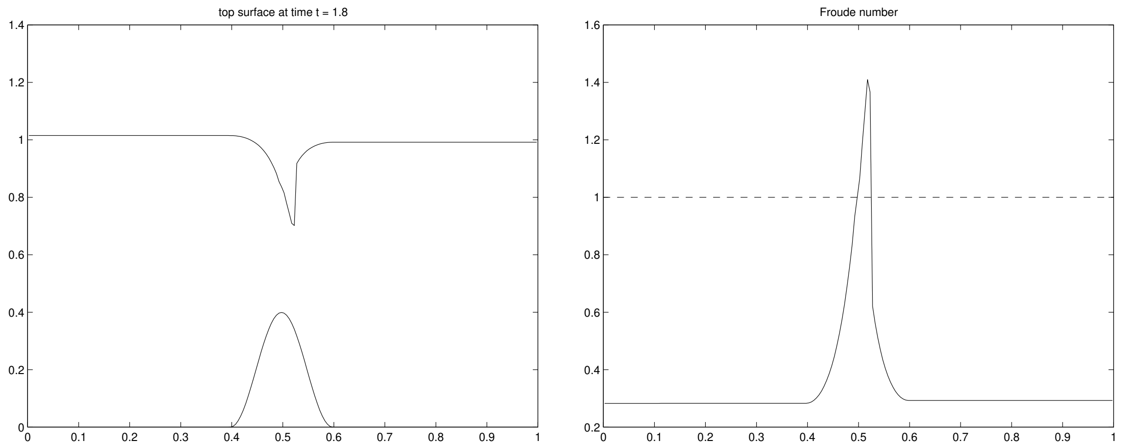

Figure 5: Transcritical flow over a ridge, where the Froude number passes through 1 and the steady-state solution contains a shock wave. Computed with the quasi-steady method after obtaining an initial approximation with a fractional step method.

discussion of flow over a ridge, consisting of an isolated hump as in the previous example. If the freestream Froude number is sufficiently small then the flow is entirely subcritical ($Fr < 1$ everywhere), while if the freestream Froude number is sufficiently large then the flow is entirely supercritical ($Fr > 1$ everywhere). In both these cases the solution is smooth and the quasi-steady method proposed here appears to work just as well as for the stationary steady state.

For intermediate freestream Froude numbers, the flow can be transcritical with transitions where Fr passes through 1, and hence one of the eigenvalues $u \pm \sqrt{gh}$ of the Jacobian passes through 0. Referring back to the case of a linear system discussed in Section 4, this would correspond to a singular matrix A. Note that in this case there exist vectors $[q]$ for which $A[q] = 0$, which means the Rankine-Hugoniot conditions can be satisified with speed 0. It is only in this singular case that the steady state solution can contain a stationary shock.

Figure 5 shows one such case, in which the freestream Froude number is less than one but the flow accelerates to a supercritical value over the hump and then decelerates through a shock wave on the lee side of the ridge. Similar solutions are seen in steady-state Euler calculations of transonic nozzles or airfoils.

Recalling the expression (14) for δ_i in the case of a linear system, it might be expected that difficulties can arise in solving for the required δ_i in the transcritical case. The solution shown in Figure 5 was computed by starting with impulsive initial data $h(x, 0) = 1 - B(x)$ and $u \equiv 0.3$ and marching forward in time. At the time when the shock first forms, nonconvergence of the Newton iteration was observed when using the quasi-steady method as described above.

Instead of using the quasi-steady method from the start, the fractional step method was used until after the shock formed and an approximate steady state was reached, at which point the quasi-steady method could be successfully used without further difficulty (in spite of the singularity of the Jacobian). It is not surprising that the fractional step approach is more robust for data that is not close to steady state. Once an approximate steady state is reached the quasi-steady method appears to work well in many, though not all, transcritical cases. This requires further study.

CLAWPACK **implementation.** This algorithm is easily implemented in the CLAWPACK software package [9] (which implements the wave-propagation algorithms) simply by changing the Riemann solver `rp1` to first solve for each δ_i and modify the left and right states before solving the Riemann problem. Riemann solvers for the 1D and 2D shallow water equations and eventually other examples can be found through

`http://www.amath.washington.edu/~rjl/clawpack/quasisteady`

6 Two space dimensions

In two space dimensions the shallow water equations take the form

$$\begin{aligned} h_t + (hu)_x + (hv)_y &= 0 && (24) \\ (hu)_t + \left(hu^2 + \frac{1}{2}gh^2\right)_x + (huv)_y &= -ghB_x && (25) \\ (hv)_t + (huv)_x + \left(hv^2 + \frac{1}{2}gh^2\right)_y &= -ghB_y. && (26) \end{aligned}$$

Again we consider the wave propagation algorithm of [11] on a finite-volume Cartesian grid, with h_{ij} representing the cell average of the depth on the (i,j) cell, for example. In the absence of source terms ($B \equiv$ const), the algorithm proceeds by solving a one-dimensional Riemann problem normal to each interface between grid cells and propagating the resulting waves into the neighboring cells. In addition to second-order correction terms, which take exactly the same form as in one dimension, the waves are also split in the orthogonal direction by solving a "transverse Riemann problem", and influence the adjacent cells in the orthogonal direction in an upwinded manner. This gives the "corner coupling" needed for improved stability and full second-order accuracy.

The algorithm is entirely unchanged when source terms are added, except that again the states used to solve the Riemann problem normal to each cell edge are not the original cell averages, but rather modified values obtained by cancelling the source terms.

Consider the interface between cells $(i-1,j)$ and (i,j), for example, where we must solve a one-dimensional Riemann problem in the x-direction. the equations solved are

$$\begin{aligned} h_t + (hu)_x &= 0 \\ (hu)_t + \left(hu^2 + \frac{1}{2}gh^2\right)_x &= -ghB_x && (27) \\ (hv)_t + (huv)_x &= 0. && (28) \end{aligned}$$

The first two equations decouple from the third are are just the one-dimensional shallow water equations with source terms considered in Section 5. The third equation is simply an advection equation for v, which propagates with speed u.

Each value h_{ij} is modified as described in Section 5, to obtain

$$h_{ij}^{\pm} = h_{ij} \pm \delta_{ij}^x,$$

where δ_{ij}^x is the modification needed to cancel the source term $-ghB_x$ in the second equation of (27). We again assume that B is known at each cell edge, and approximate $B_x \Delta x$ by $B_{i+1/2,j} - B_{i-1/2,j}$. The Riemann problem (27) is then solved with data $Q_{i-1,j}^{+}$ and Q_{ij}^{-}. The waves and flux difference resulting from this Riemann problem are used in the standard way. In particular, in the CLAWPACK implementation, only the Riemann solver `rpn2` is modified, in essentially the same way as the one-dimensional Riemann solver `rp1` is modified to implement the modification of Section 5.

Similarly, in the y-direction we solve the Riemann problem

$$\begin{aligned} h_t + (hv)_y &= 0 \\ (hu)_t + (huv)_y &= 0 \\ (hv)_t + \left(hv^2 + \frac{1}{2}gh^2\right)_y &= -ghB_y. \end{aligned} \tag{29}$$

Between cells $(i, j-1)$ and (i, j) we insteady solve the homogeneous Riemann problem with data $Q^+_{i,j-1}$ and Q^-_{ij} where now

$$h^{\pm}_{ij} = h_{ij} \pm \delta^y_{ij}$$

with δ^y_{ij} chosen so that

$$(vh)^2_{ij}\left(\frac{1}{h_{ij}+\delta^y_{ij}} - \frac{1}{h_{ij}-\delta^y_{ij}}\right) + gh_{ij}(2\delta^y_{ij} + (B_{i,j+1/2} - B_{i,j-1/2})) = 0,$$

analogous to (22).

The quasi-stationary case. Again one steady solution consists of motionless water ($u \equiv v \equiv 0$) with a flat surface, $h(x, y) = 1 - B(x, y)$. Since B is given at cell edges, the best numerical approximation to h for the undisturbed surface would be

$$h_{ij} = 1 - \frac{1}{4}(B_{i-1/2,j} + B_{i+1/2,j} + B_{i,j-1/2} + B_{i,j+1/2}).$$

Unlike the one-dimensional case, this will not in general be an exact numerical steady state using the approach introduced here, but still this approach preserves this steady state far better than a fractional step method if the bottom topography varies appreciably.

Example 6.1. The two-dimensional hump

$$B(x, y) = 0.5\exp(-50((x-0.5)^2 + (y-0.5)^2)). \tag{30}$$

is used, which has a maximum height of 0.5 at the center of the unit square. The depth is set to $h(x, y) = 1 - B(x, y)$. Table 6.1 shows the max-norm of $h - 1 + B$ at time $t = 0.1$ for the quasi-steady method and the Strang splitting on three different grids. The quasi-steady method exhibits second order accuracy whereas the Strang splitting appears to give something between first- and second-order accuracy in this case.

Accuracy tests on other problems where a perturbation to the surface is included and a fine-grid solution is used for comparison have also been performed. These indicate that the quasi-steady method does remain second-order accurate in general, in the two-dimensional case.

Example 6.2. Figure 6 shows an example analogous to the tests done previously in one dimension. The isolated hump (30) is used. The surface is initially flat with $h = 1 - B$ except for $0.05 < x < 0.15$, where h is perturbed upwards by $\epsilon = 0.01$. Figure 6 shows the right-going portion of the disturbance after it has propagated past the hump, both as mesh plots and

Table 1: Error in water surface at time $t = 0.1$ for 2D shallow water equations in the stationary case, on $N \times N$ grids.

N	Quasi-steady method	Strang splitting
50	1.1E-3	1.2E-3
100	2.8E-4	4.8E-4
200	7.0E-5	1.4E-4

contour plots. Note that the wave speed is slower above the hump than elsewhere, leading to a distortion of the initially planar disturbance.

Results obtained with the quasi-steady method on a 100×100 grid are used for reference, and the quasi-steady method and fractional step method (with the Strang splitting) are compared on 50×50 grids. They produce similar results, but the quasi-steady method clearly produces smoother and more accurate results near the location of the hump.

Acknowledgments.

This work was supported in part by NSF Grants DMS-9505021, DMS-96226645, and DOE Grant DE-FG03-96ER25292.

References

[1] A. Bermudez and M. Vazquez, *Upwind methods for hyperbolic conservations laws with source term*, Computers and Fluids, 23 (1994), pp. 1049–1071.

[2] R. Eulderink and G. Mellema, *General relativistic hydrodynamics with a Roe solver*, Astron. Astrophys. Suppl. Ser., 110 (1995), pp. 587–623.

[3] J. Falcovitz and M. Ben-Artzi, *Recent developments of the GRP method*, JSME International J. Series B, 38 (1995), pp. 497–517.

[4] H. M. Glaz and T.-P. Liu, *The asymptotic analysis of wave interactions and numerical calculations of transonic nozzle flow*, Advances Appl. Math., 5 (1984), pp. 111–146.

[5] J. Glimm, G. Marshall, and B. Plohr, *A generalized Riemann problem for quasi-one-dimensional gas flows*, Advances Appl. Math., 5 (1984), pp. 1–30.

[6] J. M. Greenberg and A. Y. LeRoux, *A well-balanced scheme for the numerical processing of source terms in hyperbolic equations*, SIAM J. Numer. Anal., 33 (1996), pp. 1–16.

[7] J. M. Greenberg, A. Y. LeRoux, R. Baraille, and A. Noussair, *Analysis and approximation of conservation laws with source terms*, SIAM J. Numer. Anal., 34 (1997), pp. 1980–2007.

[8] D. D. Houghton and A. Kasahara, *Nonlinear shallow fluid flow over an isolated ridge*, Comm. Pure Appl. Math., 21 (1968), pp. 1–23.

[9] R. J. LeVeque, CLAWPACK *software.* available from `netlib.att.com` in `netlib/pdes/claw` or on the Web at the URL `http://www.amath.washington.edu/~rjl/clawpack.html`.

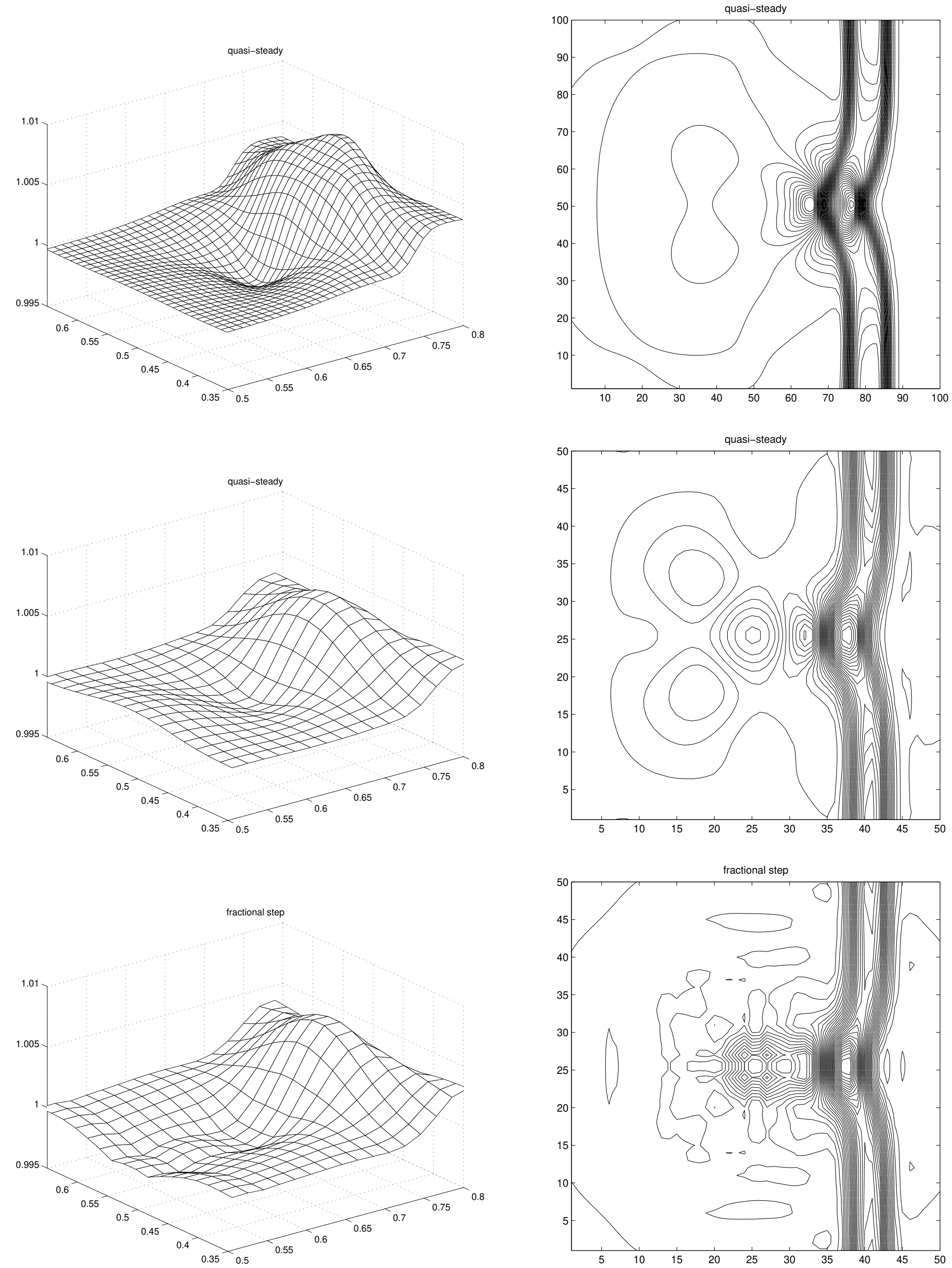

Figure 6: Two-dimensional shallow water equations. An initially planar disturbance goes over an isolate hump centered at (0.5, 0.5). Left column: mesh plots of the top surface, blown up near the center. Right column: contour plots of $h + B$, with the same contour levels in each. Top: Quasi-steady method on 100×100 grid. Middle: Quasi-steady method on 50×50 grid. Bottom: Fractional step method on 50×50 grid.

[10] R. J. LeVeque, *Numerical Methods for Conservation Laws*, Birkhäuser-Verlag, 1990.

[11] R. J. LeVeque, *Wave propagation algorithms for multi-dimensional hyperbolic systems*, J. Comput. Phys., 131 (1997), pp. 327–353.

[12] R. J. LeVeque, D. Mihalas, E. Dorfi, and E. Müller, *Numerical Methods in Astrophysical Fluid Flow*, Twenty-seventh Saas-Fee Course, (A. Gautschy and O. Steiner, editors) Springer-Verlag, to appear.
(`ftp://amath.washington.edu/pub/rjl/papers/saasfee.ps.gz`).

[13] G. Mellema, F. Eulderink, and V. Icke, *Hydrodynamical models of aspherical planetary nebulae*, Astron. Astrophys., 252 (1991), pp. 718–732.

[14] P. L. Roe, *Upwind differencing schemes for hyperbolic conservation laws with source terms*, in Nonlinear Hyperbolic Problems, C. Carraso, P.-A. Raviart, and D. Serre, eds., Springer-Verlag, Lecture Notes in Mathematics 1270, 1986, pp. 41–51.

[15] B. van Leer, *On the relation between the upwind-differencing schemes of Godunov, Engquist-Osher, and Roe*, SIAM J. Sci. Stat. Comput., 5 (1984), pp. 1–20.

[16] G. Watson, D. H. Peregrine, and E. F. Toro, *Numerical solution of the shallow-water equations on a beach using the weighted average flux method*, in Computational Fluid Dynamics '92, C. Hirsch et al., eds., Elsevier Science Publishers, 1992, pp. 495–502.